

## OPTIMAL VIBRATION CONTROL OF CONICAL SHELLS WITH COLLOCATED HELICAL SENSOR/ACTUATOR PAIRS

H. LI, S.D. HU, H.S. TZOU

*Zhejiang University, School of Aeronautics and Astronautics, StrucTronic Systems and Control Lab, Zhejiang, P.R. China  
e-mail: hstzou@zju.edu.cn; Lhlihua@gmail.com*

Z.B. CHEN

*Harbin Institute of Technology, School of Mechatronics Engineering, Harbin, P.R. China*

This paper focuses on the optimal vibration control of clamped-free conical shells using distributed helical piezoelectric sensor/actuator (S/A) pairs. Based on the independent modal space control, the response of conical shell to external excitations is represented by the summation of all participating natural modes and their respective modal participation factors, and each mode can be controlled independently. The modal equation is transformed into the linear state space form. The linear quadratic (LQ) controllers are designed for each independent mode. The optimal gain matrix is related to the ratio  $\mathbf{G}^*$  between the control voltage and sensing signal by the modal control force per unit voltage  $B_2$  and the sensing signal per unit displacement  $C_1$ . Because  $B_2$  and  $C_1$  change with locations of the S/A pair, the optimal control effects, modal control forces and corresponding optimal control voltages are evaluated using two S/A pairs at different locations. The results indicate that the optimal control method is effective in vibration control of the shell. The optimal control effect also depends on the location of the S/A pair and modal shapes as well as the modal control force and input voltage.

*Key words:* smart structure, conical shell, diagonal sensor/actuator, optimal vibration control

### 1. Introduction

Thin plates and shells laminated with active sensing and actuation layers regulated by control electronics are common configurations of smart structures and structronic systems. The laminated thin shells have desired characteristics, such as precision manipulation, light weight, highly integrated, size/energy savings, *etc.* Among commonly used smart materials, piezoelectric materials are widely used in laminated smart structures for vibration control, shape control, structural diagnosis, energy harvesting and so on (Chai *et al.*, 2004, 2006; Tzou *et al.*, 2003; Tzou and Fu, 1994). In vibration control applications, piezoelectric layers are attached to the substructure and work on both direct and converse piezoelectric effects. In the direct mode, the piezoelectric patch performs as a sensor, and the sensing signals can be used for the controller. With the converse effect, the piezoelectric patches perform as actuators, and they generate the control force for structural actuation and control (Tzou, 1993).

The conical shell is widely used in nozzles, hones, aerospace structures, submarines; for example, spacecraft adapters and noses of rockets and missiles. In these applications, conical shells are subjected to severe dynamic loads and, thus, active vibration control is necessary to protect the payload or guarantee shape precision of the shell structure. Dynamic and elastic behavior of conical shells have been investigated for decades. Leissa (1993) reviewed and summarized earlier work. Studies of vibration behavior of conical shells and conical panels as well as the

multi-layered conical shells were carried out using the kernel particle (KP) Ritz method (Liew *et al.*, 2005). Piezoelectric materials are prevalent for distributed sensing and active control of shells. The sensing signals and control actions of piezoelectric sensors and actuators are related to the location, size, shape and contributing modes. And certain vibration modes cannot be controlled by using fully distributed sensors and actuators due to the lack of observability and controllability (Tzou, 1993).

The optimal control technology, as an effective control algorithm, has been adapted to the control of beams and plates (Chellabi *et al.*, 2009; Chen and Shen, 1997; To and Chen, 2007). But the applications to distributed shell structures are still not well explored. Tzou and Ding (2004) investigated the optimal control of precision paraboloidal shell structronic systems. A linear quadratic optimal state feedback controller was designed to suppress the transverse vibrations using the independent modal control method. Ray (2003) reported the active vibration control of a shell panel using the optimal control algorithm, and found that the piezoelectric actuators need higher control voltages as the panel width (central angle) decreases to achieve equivalent control effects.

This study focuses on the optimal vibration control of conical shells using surfaced laminated revolving helical sensor/actuator pairs. Thin helical-shape sensors and actuators are collocated on both surfaces of the conical shells. This helical arrangement is used to avoid the observation of spillover. The equations of motion are given for conical shell first, followed by the derivation of modal vibration equations, and then transformed into the first-order linear state space form. The modal participation factor and its time derivative are chosen to be the state vector; the sensing signal and modal control force are chosen as the system output vector and control input respectively. The LQ controller is designed for each independent mode. The optimal gain matrix is evaluated by minimizing the performance criterion function. Then case studies are performed to evaluate the control effectiveness.

## 2. Dynamics and actuation of conical shells

Revolving helical distributed piezoelectric sensors and actuators (S/A) are laminated on the conical shell surface. In the control procedure, the dynamic response is detected by piezoelectric sensors, and the signals are subsequently used as the control input. The controller estimates the required control voltage based on the vibrational signal and then generates a control signal to the power amplifier (PA). The PA generates the accurate voltage to actuate the piezoelectric actuator. Thus, the vibration characteristics should be investigated before the controller design in the control procedure.

It is assumed that the truncated conical shell of an revolution is made of isotropic material, and the shell is thin so that the Kirchhoff-Love assumptions are applicable (Tzou, 1993). Also, since the S/A layers are much thinner than the shell structure, their mass and elasticity are negligible, and only the piezoelectric sensing/actuation effects are considered. Figure 1 shows the conical shell model in which the tri-orthogonal coordinate system  $(x, \psi, \alpha_3)$  locates on the neutral surface of the shell, where  $x$  is the longitudinal coordinate,  $\psi$  the circumferential coordinate, and  $\alpha_3$  the thickness direction. The shell is defined from  $x_1$  (minor end) to  $x_2$  (major end) in the  $x$  coordinate, and from  $-h/2$  to  $h/2$  in the  $\alpha_3$  coordinate, where  $h$  is shell thickness. The hatched area represents the helical piezoelectric S/A strips. The conical shell has semi-vertex angle  $\beta^*$ , the sensor stripe has thickness  $h^S$  and the actuator has thickness  $h^a$ .

The equations of motion for a thin circular conical shell in linear vibration are given as (Soedel, 2004)

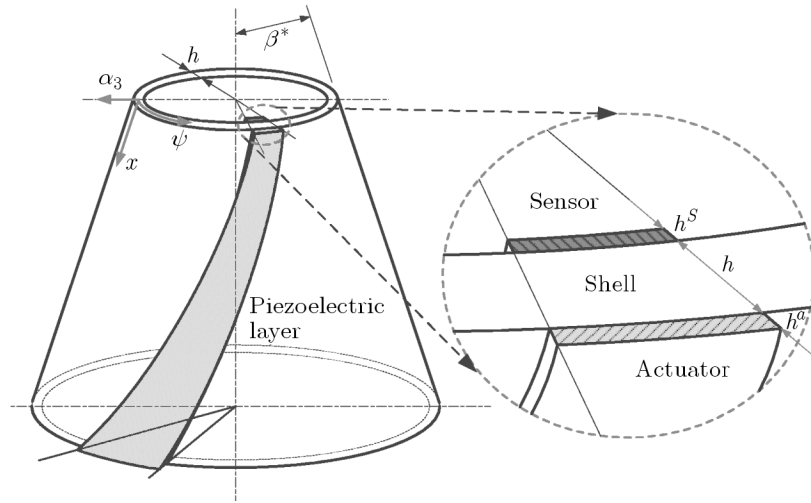


Fig. 1. Definition of conical shell with helical piezoelectric sensor/actuator

$$\begin{aligned}
 \frac{\partial N_{xx}}{\partial x} + \frac{1}{x \sin \beta^*} \frac{\partial N_{\psi x}}{\partial \psi} + \frac{1}{x} (N_{xx} - N_{\psi \psi}) + q_x &= \rho h \frac{\partial^2 u_x}{\partial t^2} \\
 \frac{\partial N_{x\psi}}{\partial x} + \frac{2}{x} N_{\psi x} + \frac{1}{x \sin \beta^*} \frac{\partial N_{\psi \psi}}{\partial \psi} + \frac{1}{x \tan \beta^*} Q_{\psi 3} + q_\psi &= \rho h \frac{\partial^2 u_\psi}{\partial t^2} \\
 \frac{\partial Q_{x3}}{\partial x} + \frac{1}{x} Q_{x3} + \frac{1}{x \sin \beta^*} \frac{\partial Q_{\psi 3}}{\partial \psi} + \frac{1}{x \tan \beta^*} N_{\psi \psi} + q_3 &= \rho h \frac{\partial^2 u_3}{\partial t^2}
 \end{aligned} \tag{2.1}$$

And the transverse shear forces  $Q_{i3}$  are defined as

$$\begin{aligned}
 Q_{x3} &= \frac{\partial M_{xx}}{\partial x} + \frac{M_{xx}}{x} + \frac{1}{x \sin \beta^*} \frac{\partial M_{\psi x}}{\partial \psi} - \frac{M_{\psi \psi}}{x} \\
 Q_{\psi 3} &= \frac{\partial M_{x\psi}}{\partial x} + \frac{2}{x} M_{\psi x} + \frac{1}{x \sin \beta^*} \frac{\partial M_{\psi \psi}}{\partial \psi}
 \end{aligned} \tag{2.2}$$

where  $N_{ij}$  and  $M_{ij}$  are the membrane forces and the bending moments respectively;  $\rho$  is the shell mass density;  $q_i$  is the mechanical load;  $u_i$  is the displacement response in the  $i$ -th direction and  $i = x, \psi, 3$ .

In the vibration analysis of conical shells, the modal expansion method is used to synthesize the dynamic response using known mode shape functions. The amount of each modal participation in the total dynamic response is defined by a modal participation factor. The total dynamic response can be represented by the summation of all participating natural modes and their respective modal participation factors (Tzou, 1993)

$$u_i(x, \psi, t) = \sum_{m=1}^{\infty} \eta_m(t) U_{im}(x, \psi) \tag{2.3}$$

where the subscript  $i = x, \psi, 3$  denotes the coordinate;  $\eta_m(t)$  is the modal participation factor;  $U_{im}(x, \psi)$  is the modal shape function of the  $m$ -th mode; and the subscript  $m = 1, 2, \dots$  of a shell continuum. Therefore, imposing the modal orthogonality, transforming shell Eqs. (2.1) into the modal coordinate and adding the modal viscous damping yields the independent modal vibration equation

$$\ddot{\eta}_m + 2\zeta_m \omega_m \dot{\eta}_m + \omega_m^2 \eta_m = F_m(t) \tag{2.4}$$

where  $\omega_m$  is the  $m$ -th natural frequency;  $\zeta_m$  is the modal damping ratio;  $F_m(t)$  is the modal force which can be decomposed into the mechanical force  $\hat{F}_m$  and control force  $\hat{F}_m^c$  and their contributing components  $(\hat{T}_m)_{i,j}$

$$F_m = \hat{F}_m + \hat{F}_m^c \quad (2.5)$$

and

$$\begin{aligned} \hat{F}_m &= \frac{1}{\rho h N_m} \int_x \int_\psi \left( \sum_{i=1}^3 q_i U_{im} \right) x \sin \beta^* d\psi dx \\ \hat{F}_m^c &= (\hat{T}_m)_{x,mem} + (\hat{T}_m)_{x,bend} + (\hat{T}_m)_{\psi,mem} + (\hat{T}_m)_{\psi,bend} \end{aligned} \quad (2.6)$$

where  $(\hat{T}_m)_{i,j}$  is the modal control force components, i.e., the longitudinal membrane and bending components  $((\hat{T}_m)_{x,mem}, (\hat{T}_m)_{x,bend})$  and the circumferential membrane and bending components  $((\hat{T}_m)_{\psi,mem}, (\hat{T}_m)_{\psi,bend})$  derived later. At the steady state, the response is also harmonic, but lagging behind by a phase angle  $\psi_m$

$$\eta_m(t) = \eta_m^* e^{j(\omega t - \psi_m)} \quad (2.7)$$

where  $j = \sqrt{-1}$ ;  $\omega$  is the frequency of excitation; and  $\eta_m^*$  is the response magnitude

$$\begin{aligned} \eta_m^* &= \frac{F_m}{\omega_m^2 \sqrt{[1 - (\omega/\omega_m)^2]^3 + 4\zeta_m^2 (\omega/\omega_m)^2}} \\ \psi_m &= \tan^{-1} \frac{2\zeta (\omega/\omega_m)}{1 - (\omega/\omega_m)^2} \end{aligned} \quad (2.8)$$

Both the modal mechanical force and the modal control force are functions of the mode shape function. The mode shape functions depends on the boundary conditions in this study, because the mode shape function should satisfy the geometrical constrains at the boundaries. Then the constants in the modal functions are solved using the Rayleigh-Ritz method. In this study, the boundary conditions are chosen to be clamped at the major end and free at the minor end, i.e., similar to a nozzle setup. The modal functions for clamped-free conical shells are further assumed as (Leissa and Kang, 1999)

$$\begin{aligned} U_{xm}(x, \psi) &= \cos(n\psi)(x - x_2) \sum_{i=0}^I A_i x^i \\ U_{\psi m}(x, \psi) &= \sin(n\psi)(x - x_2) \sum_{j=0}^J B_j x^j \\ U_{3m}(x, \psi) &= \cos(n\psi)(x - x_2) \sum_{k=0}^K C_k x^k \end{aligned} \quad (2.9)$$

where  $n$  is the circumferential wave number.  $A_i$ ,  $B_j$  and  $C_k$  are arbitrary coefficients determined by using the Rayleigh-Ritz procedure.  $I$ ,  $J$  and  $K$  are constants defining the order of the modal functions. Based on this mode shape functions, the four components, i.e., longitudinal membrane and bending components and circumferential membrane and bending components of the modal control force in Eq. (2.6)<sub>2</sub> are given as (Li et al., 2010a)

$$\begin{aligned}
(\widehat{T}_m)_{x,mem} &= -\frac{d_{31}Y_p\phi^a(t)\sin\beta^*}{\rho hN_m} \\
&\cdot \int_{x_1^*\psi_1^*}^{x_2^*\psi_2^*} \cos(n\psi)\{x[\delta(x-x_1^*)-\delta(x-x_2^*)]+1\}(x-x_2)\sum_{i=0}^I A_i x^i d\psi dx \\
(\widehat{T}_m)_{x,bend} &= -\frac{r^a d_{31}Y_p\phi^a(t)\sin\beta^*}{\rho hN_m} \int_{x_1^*\psi_1^*}^{x_2^*\psi_2^*} \cos(n\psi)\{2[\delta(x-x_1^*)-\delta(x-x_2^*)] \\
&+ x\frac{\partial}{\partial x}[\delta(x-x_1^*)-\delta(x-x_2^*)]\}(x-x_2)\sum_{k=0}^K C_k x^k d\psi dx \\
(\widehat{T}_m)_{\psi,mem} &= \frac{d_{31}Y_p\phi^a(t)}{\rho hN_m} \left\{ \sin\beta^* \int_{x_1^*\psi_1^*}^{x_2^*\psi_2^*} \cos(n\psi)(x-x_2)\sum_{i=0}^I A_i x^i d\psi dx \right. \\
&- \int_{x_1^*\psi_1^*}^{x_2^*\psi_2^*} [\delta(\psi-\psi_1^*)-\delta(\psi-\psi_2^*)]\sin(n\psi)(x-x_2)\sum_{j=0}^J B_j x^j d\psi dx \\
&+ \left. \cos\beta^* \int_{x_1^*\psi_1^*}^{x_2^*\psi_2^*} \cos(n\psi)(x-x_2)\sum_{k=0}^K C_k x^k d\psi dx \right\} \tag{2.10} \\
(\widehat{T}_m)_{\psi,bend} &= \frac{r^a d_{31}Y_p\phi^a(t)}{\rho hN_m} \left\{ \frac{-1}{\tan\beta^*} \right. \\
&\cdot \int_{x_1^*\psi_1^*}^{x_2^*\psi_2^*} [\delta(\psi-\psi_1^*)-\delta(\psi-\psi_2^*)]\sin(n\psi)\frac{x-x_2}{x}\sum_{j=0}^J B_j x^j d\psi dx \\
&+ \sin\beta^* \int_{x_1^*\psi_1^*}^{x_2^*\psi_2^*} \cos(n\psi)[\delta(x-x_1^*)-\delta(x-x_2^*)](x-x_2)\sum_{k=0}^K C_k x^k d\psi dx \\
&- \left. \frac{1}{\sin\beta^*} \int_{x_1^*\psi_1^*}^{x_2^*\psi_2^*} \cos(n\psi)\frac{\partial}{\partial\psi}[\delta(\psi-\psi_1^*)-\delta(\psi-\psi_2^*)]\frac{x-x_2}{x}\sum_{k=0}^K C_k x^k d\psi dx \right\}
\end{aligned}$$

and

$$N_m = \int_{x_1\psi_1}^{x_2\psi_2} \left( \sum_{i=1}^3 U_{im}^2 \right) x \sin\beta^* d\psi dx \tag{2.11}$$

where  $Y_p$  is Young's modulus of the piezoelectric actuator;  $r^a$  is the distance between the shell neutral surface and the mid-surface of the actuator layer;  $d_{31}$  is the piezoelectric strain constant; and  $\phi^a(t)$  is the control voltage. Assuming that the piezoelectric layer and the shell structure have a uniform thickness, and the thickness keeps identical over the actuator patch. It is assumed that only the transverse voltage  $\phi_3(x, \psi, t)$  is considered, i.e.,  $\phi^a(t) = \phi_3(x, \psi, t)$ .  $\delta(\cdot)$  is a Dirac delta function.  $x_i^*$  and  $\psi_i^*$  are locations of the S/A pair.

The modal sensing signal of the clamped-free conical shell is expressed as

$$\phi_m^S = \frac{h^S}{S^e} \int_{x_1^S}^{x_2^S} \int_{\psi_1^S}^{\psi_2^S} (h_{31} S_{xx} + h_{32} S_{\psi\psi}) x \sin \beta^* d\psi dx \quad (2.12)$$

where  $S_{xx}$  and  $S_{\psi\psi}$  are the strains of the  $m$ -th mode;  $h^S$  is the sensor thickness;  $h_{31}$  and  $h_{32}$  are piezoelectric strain constants; and  $S^e$  is the electrode area given as

$$S^e = \int_{x_1^S}^{x_2^S} \int_{\psi_1^S}^{\psi_2^S} x \sin \beta^* d\psi dx \quad (2.13)$$

Here the modal sensing signal is a time-domain response, because the strains  $S_{xx}$  and  $S_{\psi\psi}$  are functions of the modal participation factor  $\eta_m(t)$  and mode shape functions  $U_{im}(x, \psi)$ . The amplitudes of the modal strains are  $S_{xx}^*$  and  $S_{\psi\psi}^*$ , i.e.,  $S_{xx} = \eta_m(t) S_{xx}^*$  and  $S_{\psi\psi} = \eta_m(t) S_{\psi\psi}^*$ . Furthermore, the strains can be written as  $S_{xx}^* = S_{xx}^{0*} - r_x^S k_{xx}^*$  and  $S_{\psi\psi}^* = S_{\psi\psi}^{0*} - r_\psi^S k_{\psi\psi}^*$ , where  $r_i^S$  is the distance between the shell neutral surface and the mid-surface of the sensor layer. Accordingly, the sensing signal  $\phi_m^S$  can be factorized into four components, i.e., longitudinal membrane and bending components and circumferential membrane and bending components (Li et al., 2010b)

$$\phi_m^S = \phi_{x,mem}^S + \phi_{x,bend}^S + \phi_{\psi,mem}^S + \phi_{\psi,bend}^S \quad (2.14)$$

and

$$\begin{aligned} \phi_{x,mem}^S &= \eta_m(t) \frac{h_{31} h^S}{S^e} \int_{x_1^S}^{x_2^S} \int_{\psi_1^S}^{\psi_2^S} \cos(n\psi) \left( \sum_{i=0}^I (1+i) A_i x^i - x_2 \sum_{i=0}^I i A_i x^{i-1} \right) x \sin \beta^* d\psi dx \\ \phi_{x,bend}^S &= \eta_m(t) \frac{r_x^S h_{31} h^S}{S^e} \int_{x_1^S}^{x_2^S} \int_{\psi_1^S}^{\psi_2^S} \cos(n\psi) \left( \sum_{k=0}^K (k+1) k C_k x^{k-1} \right. \\ &\quad \left. - x_2 \sum_{k=0}^K k(k-1) C_k x^{k-2} \right) x \sin \beta^* d\psi dx \\ \phi_{\psi,mem}^S &= \eta_m(t) \frac{h_{32} h^S}{S^e} \int_{x_1^S}^{x_2^S} \int_{\psi_1^S}^{\psi_2^S} \left( \frac{n}{\sin \beta^*} (x - x_2) \sum_{j=0}^J B_j x^{j-1} + (x - x_2) \sum_{i=0}^I A_i x^{i-1} \right. \\ &\quad \left. + \frac{1}{\tan \beta^*} (x - x_2) \sum_{k=0}^K C_k x^{k-1} \right) \cos(n\psi) x \sin \beta^* d\psi dx \\ \phi_{\psi,bend}^S &= -\eta_m(t) \frac{h_{32} h^S}{S^e} \int_{x_1^S}^{x_2^S} \int_{\psi_1^S}^{\psi_2^S} \left( \frac{n \cos \beta^*}{\sin^2 \beta^*} (x - x_2) \sum_{j=0}^J B_j x^{j-2} + \frac{n^2}{\sin^2 \beta^*} (x - x_2) \sum_{k=0}^K C_k x^{k-2} \right. \\ &\quad \left. - \sum_{k=0}^K (k+1) C_k x^{k-1} + x_2 \sum_{k=0}^K k C_k x^{k-2} \right) \cos(n\psi) x \sin \beta^* d\psi dx \end{aligned} \quad (2.15)$$

The modal control force and sensing signal are important parameters in the controller design. The sensing signal represents the dynamic response of the structure and it is usually used as the input signal to the controller. And the modal control force equations are used by the controller to evaluate the accurate control voltage to the actuator. The system equation in the state space and the controller design are presented next.

### 3. State space equations

In this section, the modal vibration equation is transformed into the state space since the state space formulation is fundamental in modern control techniques. The performance criterion function and optimal gain matrix will be derived next.

The standard form of state space equations are given as (Tzou and Ding, 2004)

$$\dot{\mathbf{x}} = \mathbf{A}\mathbf{x} + \mathbf{B}\mathbf{u} + \mathbf{E}\mathbf{w} \quad \mathbf{y} = \mathbf{C}\mathbf{x} \quad (3.1)$$

where  $\mathbf{x}$  is the state variable vector;  $\mathbf{u}$  is the control input vector;  $\mathbf{w}$  is the external excitation vector;  $\mathbf{y}$  is the output vector;  $\mathbf{A}$ ,  $\mathbf{B}$ ,  $\mathbf{C}$  and  $\mathbf{E}$  are the system matrix, input matrix, output matrix and excitation matrix, respectively (Wang *et al.*, 2006). Here the modal participation factor and its time derivative are chosen as the state variables (Tzou and Ding, 2004)

$$\mathbf{x} = \begin{Bmatrix} \eta_m(t) \\ \dot{\eta}_m(t) \end{Bmatrix} \quad (3.2)$$

According to Eq. (2.6)<sub>2</sub>, distributed control actions induced by the distributed actuators are converted into a single modal control force  $\hat{F}_m^c$ . Therefore, the control input vector reduces into a single parameter

$$\mathbf{u} = \phi^a \quad (3.3)$$

The output vector is chosen to be the sensing signal induced by the distributed sensor related to the  $m$ -th mode

$$\mathbf{y} = \phi_m^S \quad (3.4)$$

And the modal mechanical load is chosen to be the external excitation

$$\mathbf{w} = \hat{F}_m \quad (3.5)$$

To keep consistent with Eqs. (3.1)-(3.5), the corresponding coefficient matrices  $\mathbf{B}$  and  $\mathbf{E}$  have to be reduced to be single column vectors, respectively and the matrix  $\mathbf{C}$  has to be reduced to be a single row vector.

By substituting the constant matrix and system vectors in Eqs. (3.2)-(3.5), Eq. (2.4) can be transformed into the first order linear state space form as

$$\begin{Bmatrix} \dot{\eta}_m(t) \\ \ddot{\eta}_m(t) \end{Bmatrix} = \begin{bmatrix} 0 & 1 \\ -\omega_m^2 & -2\zeta_m\omega_m \end{bmatrix} \begin{Bmatrix} \eta_m(t) \\ \dot{\eta}_m(t) \end{Bmatrix} + \begin{Bmatrix} 0 \\ B_2 \end{Bmatrix} \phi^a(t) + \begin{Bmatrix} 0 \\ 1 \end{Bmatrix} \hat{F}_m(t) \quad (3.6)$$

$$\mathbf{y} = \phi_m^S = [C_1 \quad 0] \begin{Bmatrix} \eta_m(t) \\ \dot{\eta}_m(t) \end{Bmatrix}$$

where  $B_2$  and  $C_1$  are elements of the coefficient matrix  $\mathbf{B}$  and  $\mathbf{C}$ , respectively.  $B_2$  is the control modal force generated by the piezoelectric actuator with unit control voltage. And  $C_1$  is the sensing signal generated by the piezoelectric sensor with unit modal participation factor ( $\eta_m = 1$ ).

According to Eqs. (2.6)<sub>2</sub> and (2.10), the ratio of the control force and the control input signal  $B_2$  becomes

$$B_2 = \frac{\hat{F}_m^c}{\phi^a} = \frac{1}{\phi^a} [(\hat{T}_m)_{x,mem} + (\hat{T}_m)_{x,bend} + (\hat{T}_m)_{\psi,mem} + (\hat{T}_m)_{\psi,bend}] \quad (3.7)$$

where

$$\begin{aligned}
\frac{(\widehat{T}_m)_{x,mem}}{\phi^a} &= -\frac{d_{31}Y_p \sin \beta^*}{\rho h N_m} \\
&\cdot \int_{x_1^* \psi_1^*}^{x_2^* \psi_2^*} \cos(n\psi) \{x[\delta(x-x_1^*) - \delta(x-x_2^*)] + 1\} (x-x_2) \sum_{i=0}^I A_i x^i d\psi dx \\
\frac{(\widehat{T}_m)_{x,bend}}{\phi^a} &= -\frac{r^a d_{31}Y_p \sin \beta^*}{\rho h N_m} \int_{x_1^* \psi_1^*}^{x_2^* \psi_2^*} \cos(n\psi) \{2[\delta(x-x_1^*) - \delta(x-x_2^*)] \\
&+ x \frac{\partial}{\partial x} [\delta(x-x_1^*) - \delta(x-x_2^*)]\} (x-x_2) \sum_{k=0}^K C_k x^k d\psi dx \\
\frac{(\widehat{T}_m)_{\psi,mem}}{\phi^a} &= \frac{d_{31}Y_p}{\rho h N_m} \left\{ \sin \beta^* \int_{x_1^* \psi_1^*}^{x_2^* \psi_2^*} \cos(n\psi) (x-x_2) \sum_{i=0}^I A_i x^i d\psi dx \right. \\
&- \int_{x_1^* \psi_1^*}^{x_2^* \psi_2^*} [\delta(\psi-\psi_1^*) - \delta(\psi-\psi_2^*)] \sin(n\psi) (x-x_2) \sum_{j=0}^J B_j x^j d\psi dx \\
&+ \left. \cos \beta^* \int_{x_1^* \psi_1^*}^{x_2^* \psi_2^*} \cos(n\psi) (x-x_2) \sum_{k=0}^K C_k x^k d\psi dx \right\} \\
\frac{(\widehat{T}_m)_{\psi,bend}}{\phi^a} &= \frac{r^a d_{31}Y_p}{\rho h N_m} \left\{ \frac{-1}{\tan \beta^*} \right. \\
&\cdot \int_{x_1^* \psi_1^*}^{x_2^* \psi_2^*} [\delta(\psi-\psi_1^*) - \delta(\psi-\psi_2^*)] \sin(n\psi) \frac{x-x_2}{x} \sum_{j=0}^J B_j x^j d\psi dx \\
&+ \sin \beta^* \int_{x_1^* \psi_1^*}^{x_2^* \psi_2^*} \cos(n\psi) [\delta(x-x_1^*) - \delta(x-x_2^*)] (x-x_2) \sum_{k=0}^K C_k x^k d\psi dx \\
&- \left. \frac{1}{\sin \beta^*} \int_{x_1^* \psi_1^*}^{x_2^* \psi_2^*} \cos(n\psi) \frac{\partial}{\partial \psi} [\delta(\psi-\psi_1^*) - \delta(\psi-\psi_2^*)] \frac{x-x_2}{x} \sum_{k=0}^K C_k x^k d\psi dx \right\}
\end{aligned} \tag{3.8}$$

The coefficient  $C_1$  can be derived according to the signal expressions in Eqs. (2.14) and (2.15)

$$C_1 = \frac{\phi_m^S}{\eta_m} = \frac{1}{\eta_m} (\phi_{x,mem}^S + \phi_{x,bend}^S + \phi_{\psi,mem}^S + \phi_{\psi,bend}^S) \tag{3.9}$$

where

$$\frac{\phi_{x,mem}^S}{\eta_m} = \frac{h_{31}h^S}{S^e} \int_{x_1^S \psi_1^S}^{x_2^S \psi_2^S} \cos(n\psi) \left( \sum_{i=0}^I (1+i) A_i x^i - x_2 \sum_{i=0}^I i A_i x^{i-1} \right) x \sin \beta^* d\psi dx$$

$$\begin{aligned}
\frac{\phi_{x,bend}^S}{\eta_m} &= \frac{r_x^S h_{31} h^S}{S^e} \int_{x_1^S}^{x_2^S} \int_{\psi_1^S}^{\psi_2^S} \cos(n\psi) \left( \sum_{k=0}^K (k+1) k C_k x^{k-1} \right. \\
&\quad \left. - x_2 \sum_{k=0}^K k(k-1) C_k x^{k-2} \right) x \sin \beta^* d\psi dx \\
\frac{\phi_{\psi,mem}^S}{\eta_m} &= \frac{h_{32} h^S}{S^e} \int_{x_1^S}^{x_2^S} \int_{\psi_1^S}^{\psi_2^S} \left( \frac{n}{\sin \beta^*} (x - x_2) \sum_{j=0}^J B_j x^{j-1} + (x - x_2) \sum_{i=0}^I A_i x^{i-1} \right. \\
&\quad \left. + \frac{1}{\tan \beta^*} (x - x_2) \sum_{k=0}^K C_k x^{k-1} \right) \cos(n\psi) x \sin \beta^* d\psi dx \\
\frac{\phi_{\psi,bend}^S}{\eta_m} &= -\frac{h_{32} h^S}{S^e} \int_{x_1^S}^{x_2^S} \int_{\psi_1^S}^{\psi_2^S} \left( \frac{n \cos \beta^*}{\sin^2 \beta^*} (x - x_2) \sum_{j=0}^J B_j x^{j-2} + \frac{n^2}{\sin^2 \beta^*} (x - x_2) \sum_{k=0}^K C_k x^{k-2} \right. \\
&\quad \left. - \sum_{k=0}^K (k+1) C_k x^{k-1} + x_2 \sum_{k=0}^K k C_k x^{k-2} \right) \cos(n\psi) x \sin \beta^* d\psi dx
\end{aligned} \tag{3.10}$$

Once the coefficient matrices **A**, **B**, **C** and **E** are known, the task left is to determine the optimal controller **u** so as to minimize the objective quadric function.

#### 4. Optimal control

In this section, the focus is on the development of an optimal control law with the helical distributed piezoelectric S/A pair. The objective is to determine the control input functions that minimize the performance criterion given by

$$J = \int_0^{\infty} [\mathbf{x}^T \mathbf{Q} \mathbf{x} + \mathbf{u}^T \mathbf{R} \mathbf{u}] dt \tag{4.1}$$

where **Q** is the state weighting matrix, **R** is the control weighting matrix, both are real symmetric, positive-definite. Generally, to achieve quick vibration suppression, a larger value of the state weight matrix should be chosen. Also, to reduce the energy consumption, a larger value of **R** matrix should be chosen (Sethi and Song, 2005). **G** is the optimal gain matrix (usually diagonal). The superscript T denotes the matrix transpose. **u** is the control input vector defined, in the controller design, the control input vector is usually written as

$$\mathbf{u} = -\mathbf{G} \mathbf{x} \tag{4.2}$$

here **G** is the optimal controller gain. This gain is a main parameter in active control and it is a function of the control weighting matrix **R**, system input vector **B** and the matrix **M**

$$\mathbf{G} = \mathbf{R}^{-1} \mathbf{B}^T \mathbf{M} \tag{4.3}$$

where the matrix **M** is the solution to the Riccati equation

$$\mathbf{M} \mathbf{A} + \mathbf{A}^T \mathbf{M} - \mathbf{M} \mathbf{B} \mathbf{R}^{-1} \mathbf{B}^T \mathbf{M} + \mathbf{Q} = \mathbf{0} \tag{4.4}$$

In this Riccati equation, the coefficient matrices  $\mathbf{Q}$  and  $\mathbf{R}$  are the weighting matrix in Eq. (4.1). When  $\mathbf{Q}$  and  $\mathbf{R}$  are specified, the matrix  $\mathbf{M}$  can be evaluated. The state weighting matrix is chosen as

$$\mathbf{Q} = \begin{bmatrix} 1 & 0 \\ 0 & Q_{22} \end{bmatrix} \quad (4.5)$$

where  $Q_{22}$  is the state weighting coefficient. According to Eq. (3.3), the control input vector reduces to a single parameter. Therefore, the control weighting matrix  $\mathbf{R}$  in Eq. (4.1) reduces to a single parameter  $R$ .

As mentioned before, in the distributed control of shell vibrations, the sensing signal from the sensor in the helical S/A pair is used as the feedback signal. The optimal controller calculates the control voltage according to the sensing signals

$$\mathbf{u} = \phi^a = -\mathbf{G}^* \begin{Bmatrix} \phi_m^S \\ \dot{\phi}_m^S \end{Bmatrix} = -\mathbf{G}^* C_1 \begin{Bmatrix} \eta_m(t) \\ \dot{\eta}_m(t) \end{Bmatrix} = -C_1 \mathbf{G}^* \mathbf{x} \quad (4.6)$$

here  $\mathbf{G}^*$  is the gain between the control input  $\mathbf{u}$  to the sensing signal  $\phi_m^S$  and its time derivative  $\dot{\phi}_m^S$ . From Eqs. (4.2) and (4.6), one derives the relation between  $\mathbf{G}$  and  $\mathbf{G}^*$  written as

$$\mathbf{G}^* = \frac{1}{C_1} \mathbf{G} \quad (4.7)$$

This optimal control scheme of conical shells using the revolving helical S/A pair is demonstrated in case studies presented next.

## 5. Case studies

In this section, the optimal control of independent modes of a clamped-free conical shell is investigated by the use of the foregoing algorithm. The conical shell model is made of Plexiglas material. The hexagonal piezoelectric material polyvinylidene-fluoride (PVDF) is used for the sensors and actuators, then  $d_{31} = d_{32}$  and  $h_{31} = h_{32}$ . (Note that the generic mathematical model and derivations can account for various shell and piezoelectric materials.) The helical S/A strips are divided into 10 segments or ten S/A pairs; each has its respective electrodes, as shown in Fig. 2. And the locations of the S/A pairs are defined as

$$x_1 + \frac{i-1}{10}(x_2 - x_1) < x < x_1 + \frac{i}{10}(x_2 - x_1) \quad i = 1, 2, 3, \dots, 10$$

$$\frac{x - x_2}{x_1 - x_2} \alpha^* - \frac{w}{2} < \psi < \frac{x - x_2}{x_1 - x_2} \alpha^* + \frac{w}{2}$$

where  $\alpha^* = \pi/4$  is the orientation angle of the diagonal strips in the circumferential direction and  $w$  is their width. The structural and material parameters are listed in Table 1.

Four cases are performed to evaluate the controller of the clamped-free conical shell: case 1 – optimal control of mode (1,2); case 2 – optimal control of mode (2,2); case 3 – optimal control of mode (1,3); and case 4 – optimal control of mode (2,3). The parameters in the modal functions are chosen as  $I = J = K = 4$ . It is assumed that:

- 1) no external mechanical excitation is applied to the shell,
- 2) the structural damping effect of the conical shell is 1% for each mode,
- 3) the initial velocity is 0 m/s,
- 4) the initial displacement of the reference point is 0.001 m.

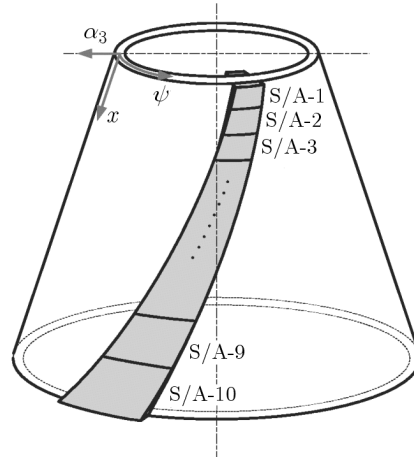


Fig. 2. Locations of S/A pair segments

**Table 1.** Geometry and material properties of the conical shell control system

Parameters	Plexiglas shell	PVDF layer	Units
Location	$x_1 = 0.2$	–	m
	$x_2 = 0.5$	–	m
Semi-vertex angle	$\beta^* = \pi/4$	–	rad
Thickness	$h = 2 \cdot 10^{-3}$	$h^S = h^a = 0.5 \cdot 10^{-3}$	m
Width	–	$w = 0.2$	rad
Young's modulus	$Y = 3.1 \cdot 10^9$	$Y_p = 2.0 \cdot 10^9$	N/m <sup>2</sup>
Poisson's ratio	$\mu = 0.3$	–	–
Mass density	$\rho = 1190.0$	$\rho_p = 1800.0$	kg/m <sup>3</sup>
Piezoelectric const.	–	$h_{31} = 4.32 \cdot 10^8$	V/m
	–	$d_{31} = 2.3 \cdot 10^{-11}$	C/N

The reference points used in the four cases are the points on the shell surface where the vibrational displacement amplitude gets the maximal value. The corresponding initial modal participation factors are evaluated via dividing the initial displacements by the modal shape functions. The snap-back response is used to evaluate the shell control effectiveness.

To enhance the vibration control, the S/A segment at the optimal location is chosen for the vibration control for each mode. Also, S/A-2 is chosen in the optimal control of each mode. The selected S/A segments are listed in Table 2.

**Table 2.** S/A segments chosen for the specific modal control

$m$	$n$	
	2	3
1	No. 2 and 5	No. 2 and 5
2	No. 2 and 9	No. 2 and 9

In the four cases, the control performances of both S/A segments are evaluated. The optimal controllers are firstly designed to satisfy the expected control performances and control voltage requirements. In this case, the control input weighting coefficient  $R$  is chosen to be 1. The state weighting matrix  $\mathbf{Q}$  is set as a diagonal positive-definite matrix, where  $Q_{11} = 1$  and  $Q_{22}$  is the design parameter of the optimal controller with the expected efficiency and cost.  $Q_{22}$  is evaluated using the following empirical equation

$$Q_{22} = [q_1 + q_2 \cos(q_3 \omega_{m,n}) + q_4 \sin(q_3 \omega_{m,n})] \sqrt{|B_{2,mn}^{Opt} / B_{2,mn}^{SA2}|}$$

where

$$q_1 = 5.72 \cdot 10^4 \quad q_2 = -2.20 \cdot 10^4 \quad q_3 = 2.36 \cdot 10^{-3} \quad q_4 = -7.57 \cdot 10^4$$

and  $B_{2,mn}^{Opt}$  is the ratio of the control force and the control input signal of the optimal S/A segment; and  $B_{2,mn}^{SA2}$  is the ratio of the control force and the control input signal of the S/A-2 segment. Generally, higher control voltage results in better vibration suppression effects, but high voltage may lead to overload or damage to the control system. And this empirical equation is chosen to avoid the overload and to guarantee the control effects.

### Case 1: Optimal control of mode (1,2)

The time domain displacement responses of the conical shell, control voltages, damping ratio and optimal gains  $\mathbf{G}^*$  are solved for each S/A segment. Figure 3 shows the displacement response of the reference point with respect to time for mode (1,2). The thin solid line is the displacement response of the conical shell without control; the dashed line is the displacement response with the optimal control using S/A-2; and the thick solid line is the displacement response with the optimal control using the optimal S/A segments (No. 5). In this mode, the optimal controller is effective to vibration control, and the optimal S/A segment generates more damping. The modal ratio using S/A-2 is 0.317%, and the damping ratio using the optimal S/A segment is 0.47%. The optimal gain  $\mathbf{G}^*$  of S/A-2 is [2.62E-9, 30.3], and it is [1.07E-9, 9.92] for the optimal S/A segment. Figure 4 shows the control voltages for both S/A segments.

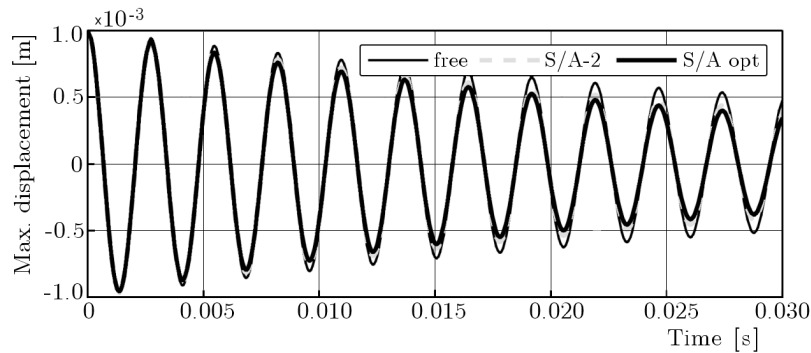


Fig. 3. Displacement response of (1,2) mode using S/A-2 and S/A-5 (optimal)

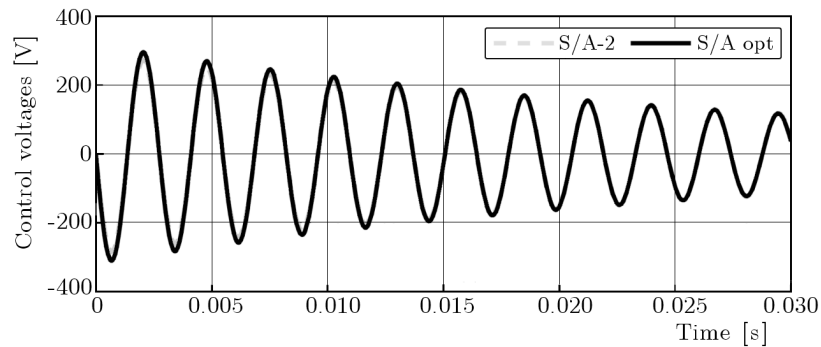


Fig. 4. Control voltages of S/A-2 and S/A-5 (optimal), mode (1,2)

### Case 2: Optimal control of mode (2,2)

In the control of mode (2,2), the optimal S/A segment (No. 9) is much more effective than S/A-2, as shown in Fig. 5. The displacement response of the conical shell reduces to zero at  $t = 0.025$  s using the optimal S/A-9, and the modal damping ratio is 4.74%. S/A-2 generates a damping ratio of 0.120%. The optimal gain  $\mathbf{G}^*$  for S/A-2 is  $[1.06\text{E-}8, 26.3]$ , and it is  $[9.73\text{E-}9, 2.61]$  for the optimal S/A-9. At mode (2,2), the control voltages for S/A-2 and the optimal S/A have opposite phases, as shown in Fig. 6. This is because that the two S/A segments have different locations. At this mode, the optimal S/A generate a positive actuation force (extensional modal control force) while applying positive voltage, but S/A-2 generates a negative modal control force (shrink force) with the same voltage. Therefore, to generate the same control effects, the S/A segments need opposite control voltage.

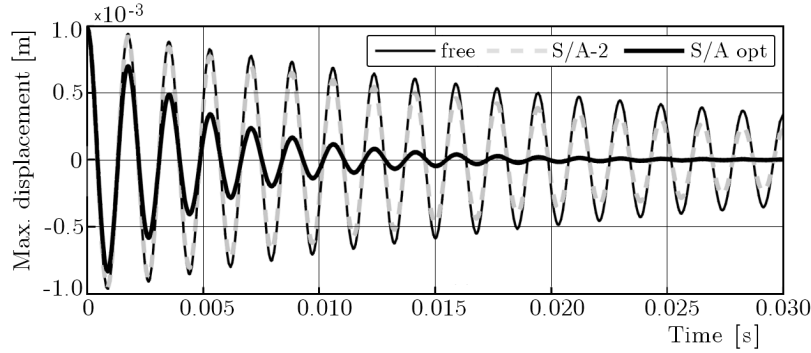


Fig. 5. Displacement response of (2,2) mode using S/A-2 and S/A-9 (optimal)

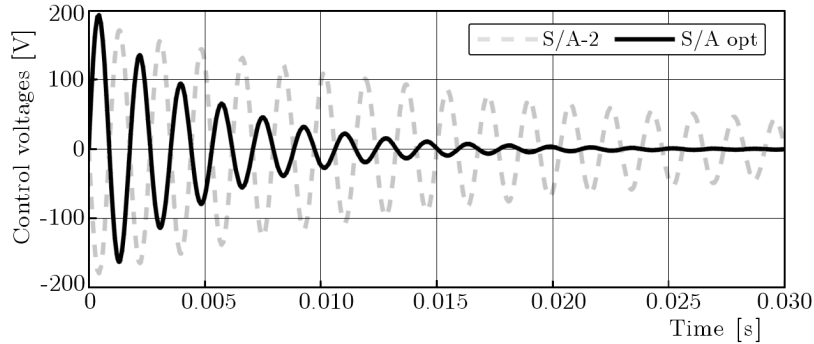


Fig. 6. Control voltages of S/A-2 and S/A-9 (optimal), mode (2,2)

### Case 3: Optimal control of mode (1,3)

At mode (1,3), the modal damping ratio of optimal S/A segments is 2.29%, the modal damping ratio of S/A-2 is 0.948%, but the control voltage of the optimal S/A-5 is lower than the voltage of S/A-2, as shown in Figs. 7 and 8. The optimal gain  $\mathbf{G}^*$  of S/A-2 is  $[2.84\text{E-}9, 21.3]$ , and it is  $[-1.75\text{E-}8, -59.2]$  for the optimal S/A-9.

### Case 4: Optimal control of mode (2,3)

Figure 9 shows the displacement response of the conical shell at mode (2,3). The optimal S/A reduces the vibration to zero at  $t = 0.03$  s, and the modal damping ratio is 4.94%. The modal damping ratio of S/A-2 is 1.11%. The optimal gain  $\mathbf{G}^*$  of S/A-2 is  $[3.51\text{E-}8, 67.7]$ , and the optimal gain  $\mathbf{G}^*$  for the optimal S/A-9 is  $[1.81\text{E-}8, 7.25]$ . But the control voltage of S/A-9

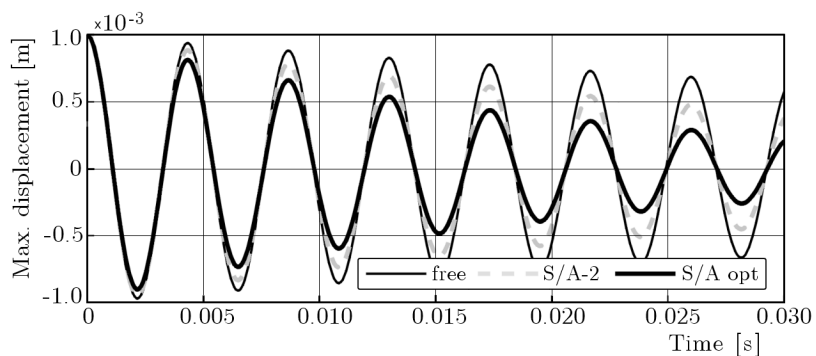


Fig. 7. Displacement response of (1,3) mode using S/A-2 and S/A-5 (optimal)

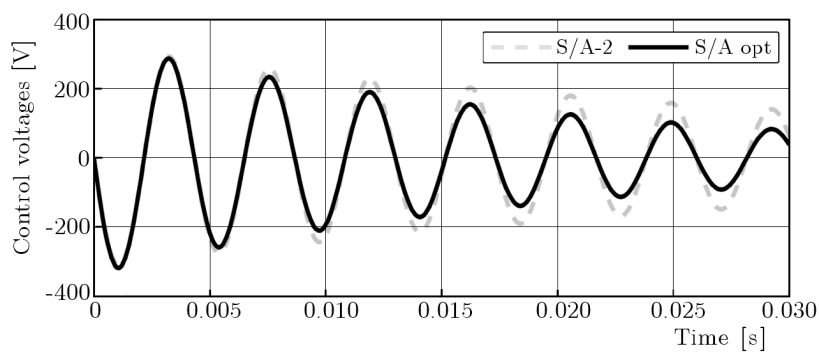


Fig. 8. Control voltages of S/A-2 and S/A-5 (optimal), mode (1,3)

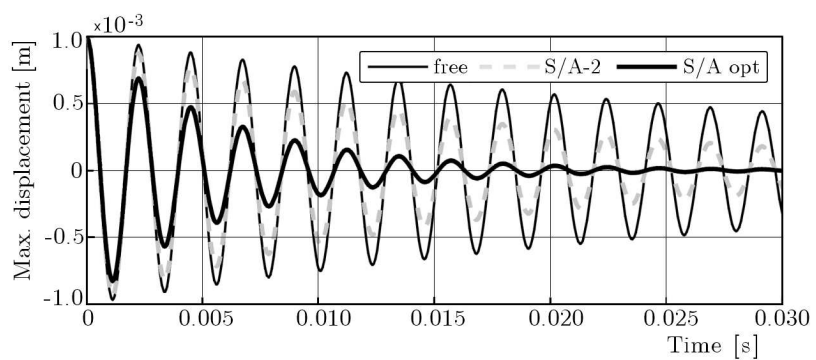


Fig. 9. Displacement response of (2,3) mode using S/A-2 and S/A-9 (optimal)

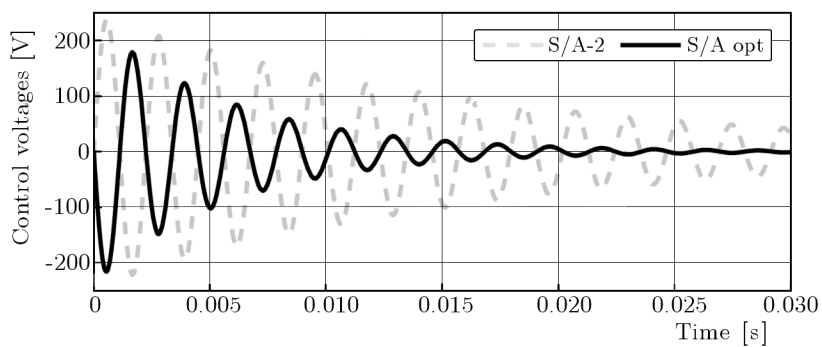


Fig. 10. Control voltages of S/A-2 and S/A-9 (optimal), mode (2,3)

is a little less than the voltage of S/A-2, as shown in Fig. 10. At this mode, the control voltages of the two S/A segments have opposite phases, for the same reason at mode (2,2).

The proposed optimal controller is effective in the vibration control of conical shell using different S/A segments. But the control performance mainly depending on the S/A location and the mode shape. In the numerical case, the S/A-5 is more effective than others in  $m = 1$  modes. S/A-5 suppresses the vibration more quickly and generates a higher modal damping ratio while the control voltages are close to each other. In  $m = 2$  modes, S/A-9 at the major end is more effective. For all evaluated modes, the element  $G_1^*$  is far less than the element  $G_2^*$  of the optimal gain  $\mathbf{G}^*$ . This reveals that the control voltage solved by the optimal controller is mainly related to the modal velocity  $\dot{\eta}$ . The overall control effects depending on the S/A locations, modes and the control voltage. To get best control effects, the optimal actuator is desired when the control voltage is given.

## 6. Conclusions

This study focused on the optimal control of conical shells using distributed revolving helical piezoelectric sensors and actuators. The helical piezoelectric strips were used as the sensors and actuators; the sensor strip was laminated on the inner surface of the conical shell and the actuator strip was laminated on the outer surface. The actuation and sensing equations of the helical sensors and actuators were given and the dynamic equations were translated into modal equation. The modal participation factor and its time differential were chosen as the system state vector, and the state space equation of the vibration equation was established. The optimal controller was derived using a linear quadratic regulator with output feedback.

Four cases were performed to evaluate the controller at four modes of the clamped-free conical shell. In each case, two S/A segments or pairs (S/A-2 and the optimal S/A pair) were chosen to study the performance differences of different S/A segments. For the same controller or control voltage, the control effects are related to the location of the S/A segments and modes. The optimal S/A segment is No. 5 in the middle of the conical shell for  $m = 1$  modes; for  $m = 2$  modes the optimal S/A segment is No. 9 at the major end. The optimal control voltage is mainly related to the modal velocity. Therefore, the S/A locations for each mode as well as the weighting matrix and modal control force should be considered in the controller design for effective vibration control of shells.

### Acknowledgments

This work was supported by China Postdoctoral Science Foundation (No. 20110491787) and the National Natural Science Foundation of China (No. 11102182 and 11172262).

## References

1. CHAI W.K., HAN Y., HIGUCHI K., TZOU H.S., 2006, Micro-actuation characteristics of rocket conical shell sections, *Journal of Sound and Vibration*, **293**, 1/2, 286-298
2. CHAI W.K., SMITHMAITRIE P., TZOU H.S., 2004, Neural potentials and micro-signals of non-linear deep and shallow conical shells, *Mechanical Systems and Signal Processing*, **18**, 4, 959-975
3. CHELLABI A., STEPANENKO Y., DOST S., 2009, Direct optimal vibration control of a piezoelectric plate, *Journal of Vibration and Control*, **15**, 7, 1093-1118
4. CHEN C.Q., SHEN Y.P., 1997, Optimal control of active structures with piezoelectric modal sensors and actuators, *Smart Materials and Structures*, **6**, 4, 403-409
5. LEISSA A.W., 1993, *Vibration of Shells*, Reprint ed., Acoustical Society of America, Sewickley

6. LEISSA A.W., KANG J.H., 1999, Three-dimensional vibration analysis of thick shells of revolution, *Journal of Engineering Mechanics – ASCE*, **125**, 12, 1365-1371
7. LI H., CHEN Z.B., TZOU H.S., 2010a, Distributed actuation characteristics of clamped-free conical shells using diagonal piezoelectric actuators, *Smart Materials and Structures*, **19**, 11, 115015
8. LI H., CHEN Z.B., TZOU H.S., 2010b, Torsion and transverse sensing of conical shells, *Mechanical Systems and Signal Processing*, **24**, 7, 2235-2249
9. LIEW K.M., NG T.Y., ZHAO X., 2005, Free vibration analysis of conical shells via the element-free kp-Ritz method, *Journal of Sound and Vibration*, **281**, 3/5, 627-645
10. RAY M.C., 2003, Optimal control of laminated shells using piezoelectric sensor and actuator layers, *AIAA Journal*, **41**, 6, 1151-1157
11. SETHI V., SONG G., 2005, Optimal vibration control of a model frame structure using piezoceramic sensors and actuators, *Journal of Vibration and Control*, **11**, 5, 671-684
12. SOEDEL W., 2004, *Vibrations of Shells and Plates*, 3 ed., Marcel Dekker Inc., New York
13. TO C.W.S., CHEN T., 2007, Optimal control of random vibration in plate and shell structures with distributed piezoelectric components, *International Journal of Mechanical Sciences*, **49**, 12, 1389-1398
14. TZOU H.S., 1993, *Piezoelectric Shell-Distributed Sensing and Control of Continua*, Kluwer Academic Publishers, Boston/Dordrecht
15. TZOU H.S., CHAI W.K., WANG D.W., 2003, Modal voltages and micro-signal analysis of conical shells of revolution, *Journal of Sound and Vibration*, **260**, 4, 589-609
16. TZOU H.S., DING J.H., 2004, Optimal control of precision paraboloidal shell structronic systems, *Journal of Sound and Vibration*, **276**, 1/2, 273-291
17. TZOU H.S., FU H.Q., 1994, A study of segmentation of distributed piezoelectric sensors and actuators, Part I: Theoretical analysis, *Journal of Sound and Vibration*, **172**, 2, 247-259
18. WANG S.Y., TAI K., QUEK S.T., 2006, Topology optimization of piezoelectric sensors/actuators for torsional vibration control of composite plates, *Smart Materials and Structures*, **15**, 2, 253-269

### Optymalne sterowanie drganiami powłok stożkowych za pomocą spiralnego skołokowanego układu czujnika i elementu wykonawczego

#### Streszczenie

W pracy skoncentrowano się na problemie optymalnego sterowania drganiami jednostronnie zamocowanych powłok stożkowych za pomocą spiralnie ułożonego układu piezoelektrycznego czujnika skołokowanego z elementem wykonawczym (S/A). W oparciu o wyniki płynące z rozwiązania przestrzennego zagadnienia sterowania modalnego, dynamiczną odpowiedź powłoki na wymuszenie zewnętrzne wyrażono sumą postaci własnych, jednocześnie stwierdzając, że można niezależnie ingerować w poszczególne postaci własne układu. Równanie modalne przetransformowano do liniowej formuły stanu. Zaprojektowano sterowniki liniowo-kwadratowe (LQ) niezależnie dla każdej postaci własnej. Optymalną macierz współczynników wzmocnienia skorelowano z transmitancją  $\mathbf{G}^*$  pomiędzy napięciem sterowania i sygnału czujnika poprzez jednostkową siłę sterującą odniesioną do napięcia  $B_2$  oraz sygnału czujnika w stosunku do przemieszczenia  $C_1$ . Ponieważ  $B_2$  i  $C_1$  zmieniają się wraz ze zmianą położenia skołokowanych par S/A, przeprowadzono ewaluację modalnych sił sterujących i odpowiadających im napięć dla różnych położenia układu sterowania. Wyniki badań potwierdziły efektywność optymalnego sterowania drganiami powłoki stożkowej. Zauważono także wrażliwość uzyskanego stopnia sterowania na położenie pary czujnika i elementu wykonawczego oraz wartości modalnej siły sterującej, jak i napięcia.